Appl Phys A
DOI 10.1007/s00339-011-6754-9

Applied Physics A
Materials Science & Processing

Quantitative studies of long-term stable, top-down fabricated silicon nanowire pH sensors

Sun Choi · Inkyu Park · Zhao Hao · Hoi-Ying N. Holman · Albert P. Pisano

Received: 17 August 2011 / Accepted: 19 December 2011

Abstract We report a simple and effective method to develop long-term stable, top-down fabricated silicon nanowire (SiNW) pH sensors along with systematic studies on the performance of the sensors. In this work, we fabricated the SiNW pH sensors based on top-down fabrication processes. In order to improve the stability of the sensor performance, the sensors were coated with a passivation layer (PECVD-based silicon nitride) for effective electrical insulation and ion-blocking. The stability, pH sensitivity, and repeatability of the sensor response are critically analyzed with regard to the physics of sensing interface between sample liquid and the sensor surface. Also, trade-off between the stability and pH sensitivity of the sensor response is discussed.

1 Introduction

Silicon nanowires (SiNW) are good sensing materials for the highly sensitive detection of chemical (ex. pH level, metal ions) and biological (ex. DNA and protein) species due to their high surface-to-volume ratio and high chemical reactivity at the surface [1–9]. Conventionally, SiNW have been synthesized chemically by Vapor–Liquid–Solid (VLS) methods and integrated with pre-patterned microscale electrodes in order to form sensor structures [1, 2, 4, 6–14]. This bottom-up approach has advantages such as good controllability of chemical and electrical properties and easy fabrication of ultrathin, single-crystalline nanowires ($\lesssim$20 nm) with atomically flat surfaces. However, there is a fundamental limitation in the integration of high-density, individually addressable array of nanowires on a single chip because it is challenging to manipulate single nanowires and pattern them in desired locations. Recently, top-down fabricated SiNW sensors have been developed by combining electron-beam lithography (EBL) with conventional photolithography [3–5, 9]. These sensors are highly favored in modern Integrated Circuit (IC) technology because the dimensions and the electrical properties of the SiNW can be easily tuned and the entire fabrication processes are CMOS (Complementary Metal-Oxide Semiconductor) process-compatible. So far, previous works on SiNW sensors have been primarily focused on the studies on the sensitivity, response time of sensors [3, 4, 13], or computational modeling of surface charge effect on the sensors [3]. Although long-term stability of SiNW sensors has been briefly discussed in our previous work [9], there has been no approach explored to improve the stability of SiNW sensors. In order for SiNW sensors to be used in industrial applications or in biomonitoring for long-term period, it is crucial to implement reliable and systematic ways to improve the stability of the sensors. Herein, we introduce a straightforward way to develop long-term, stable SiNW pH sensors. We fabricated SiNW sensors by using EBL and photolithography, which are major techniques for top-down fabrication. A passivation layer (silicon

S. Choi (✉) · A.P. Pisano
Berkeley Sensor and Actuator Center (BSAC), University of California at Berkeley, Berkeley, CA 94720, USA
e-mail: sunchoi@eecs.berkeley.edu
Fax: +1-510-6436637

S. Choi · Z. Hao · H.-Y.N. Holman
Ecology Department, Earth Sciences Division, Lawrence Berkeley National Laboratory, University of California at Berkeley, 406 Cory Hall, Berkeley, CA 94720, USA

I. Park (✉)
Department of Mechanical Engineering, Korea Advanced Institute of Science and Technology (KAIST), 291 Daehak-ro, Yoosung-Gu, Daejeon, Korea 305-701
e-mail: inkyu@kaist.ac.kr
Fax: +82-42-3503210

Published online: 05 January 2012

nitride by PECVD process) is coated on the surface of SiNW to enhance electrical insulation and ion-blocking properties of the sensor. The stability, pH sensitivity, and repeatability of the sensor response are characterized and interpreted.

2 Experimental methods

2.1 Materials

Silicon on insulator (SOI) wafer (top device layer: silicon, 100 nm; buried insulation layer: oxide, 400 nm; base substrate: silicon, 600 μm; Soitec) was used as a substrate and device structure. Leaded chip carriers (LDCC) (40 leads, Spectrum Semiconductor Materials, Inc.) and plastic leaded chip carriers (PLCC) package (Spectrum Semiconductor Materials, Inc.) were used as packaging platforms for electrical connection. PDMS (Alfa Aesar) was used as a material for microfluidic channel. Ag/AgCl reference electrode (Microelectrode, Inc.) was used to maintain the reference electrical potential between fluid and device. Buffer solution (pH 4–9) with hydrochloric acid and potassium hydroxide (Sigma-Aldrich) were used for pH measurement. In the buffer, no other ions were contained for accurate calibration.

2.2 Fabrication of silicon nanowire pH sensors

The SOI wafer was oxidized to form a thin SiO_2 of 110-nm thickness via dry thermal oxidation. It resulted in the decrease of top Si layer thickness from 100 to 50 nm. Then, the Si device layer was doped with boron (B) by ion implantation (dose $= 3.63 \times 10^{13}$ cm^{-2}; ion energy $= 18$ keV; tilt angle $= 7°$) and rapid thermal annealing at 984°C for 20 seconds in nitrogen environment was followed for dopant activation. The effective doping concentration was measured to be equivalent to 2–3 $\times$ 10^{18} cm^{-3} at the Si device layer. Afterwards, the top SiO_2 layer was thinned down to 50 nm by wet etching in 10:1 buffered oxide etchant (BOE) and PMMA was coated on the substrate (thickness $=$ 60 nm). EBL was carried out on PMMA-coated substrate to define the dimension of silicon nanowires (width: 100 nm; length: 60 μm) with an area dose of 300 μC cm^{-2}, a working distance of 4 mm and an acceleration voltage of 100 KeV. Then, the sample was developed in the PMMA developer (isopropyl alcohol (IPA):methyl isobutyl ketone (MIBK) $=$ 3:1) for 2 minutes, soaked in IPA for 1 minute, and finally rinsed with DI water. After the development, 15 nm chromium (Cr) was deposited on the sample and nanopattern was generated by lift-off process. The Cr layer was used as an etching mask for SiO_2 layer during reactive ion etching (RIE) processes in a $CF_4 + O_2$ environment, after which Cr etching mask was removed by wet Cr etchant. For the etching of Si device layer, an RIE process with $CF_4 + O_2$ gases was used. Then, the top remaining SiO_2 layer was removed by 10:1 BOE. After this, silicon nitride passivation layer was deposited on the entire substrate by Plasma Enhanced Chemical Vapor Deposition (PECVD). Metal contact area was defined by photolithography and the removal of silicon nitride passivation layer on exposed area was followed by 10:1 buffered hydrofluoric oxide etchant to remove any possible remaining silicon oxide in the contact area. Aluminum electrode was fabricated by thermal evaporation and lift-off processes. Then, the sample was thermally annealed in a forming gas (10% H_2/90% N_2) at 400°C for 30 minutes to form ohmic contact between silicon device layer and aluminum contact pads.

2.3 Packaging of silicon nanowire pH sensors

A PDMS microfluidic channel (width $=$ 50 μm; height $=$ 50 μm) was bonded to a 1 cm $\times$ 1 cm chip where SiNW pH sensor was already fabricated. The PDMS channel was aligned accurately so that the metal interconnections (Al electrodes) of the sensor chip were separated from the fluid to avoid electrical leakage between electrodes during the electrical measurement. Afterwards, the microfluidic chip was bonded to LDCC by conductive carbon tape (Ted Pella, Inc.) and gold-wire bonding was achieved between the electrodes of the sensor chip and the electrical pads in the LDCC. The LDCC was inserted to a PLCC package, which was then mounted on an electrical breadboard.

2.4 Measurement of stability of silicon nanowire pH sensors

Four-point method was used to monitor the change of the resistance of SiNW over 3 hours. AC voltage (sine wave, $V_{pp} = 100$ mV, and frequency $=$ 30 Hz) was supplied to the sensor. The output voltage across the SiNW sensor was acquired by data acquisition board and LabView interface. There exist many different ways to characterize signal disturbance in semiconductor physics [15, 16]. In this paper, two parameters, short-term-noise and long-term-drift levels, were used to quantify the disturbance to the measurement signals. Noise level was simply defined by (Averaged absolute value of the deviation of response signal from the absolute average of 10,000 data points)/(Absolute average value of the signal of 10,000 data points). Drift level was simply defined by ((Average response signal of last 30-minute measurement) − (Average response signal of initial 30-minute measurement))/(Average value of the signal for the entire measurement period). The response plot was obtained by normalizing real-time response with initial sensor response.

2.5 Measurement of pH sensitivity of silicon nanowire sensors

In order to characterize the conductance of SiNW, current–voltage (I-V) curve was obtained in the voltage range from −0.1 to 0.1 V, from which the slope of the curve was calculated by least-square fitting. The pH of the fluid sample was measured three times for each pH measurement and averaged. The error bars are included in each pH measurement graph. Most of error bars are too short to be visible in Fig. 3, however included.

For the sensitivity measurement, an I-V scanning was performed after 5 minutes of the fluid injection into PDMS microchannel in order to eliminate the flow rate effect and instability of sensor signals. Recently, the flow rate of the charged fluid was reported to be a significant factor to affect the electrical measurement of the fluid [11]. Therefore, it is important to stabilize the fluid during the measurement period in order to observe the pure contribution of pH level to the sensor response. Also, Ag/AgCl reference electrode was located at the inlet region of a microfluidic channel to maintain electrical potential between the fluid and the device.

3 Operating principle of silicon nanowire-based pH sensors

The pH detection of fluid sample was achieved based on the principle of field effect transistor (FET). As shown in Fig. 1, the outer surface of p-type SiNW is protonated in lower pH solution. The Fermi level difference between the mobile carrier (holes, p-type) channel and the outer surface induces downward bending of flat band energy near the surface and depletion layer is generated in the channel near the surface [16, 17]. By the same principle, the outer surface of SiNW is deprotonated in higher pH solution and upward bending of the energy band is induced to generate the accumulation layer of the mobile charge carriers in the channel. A passivation layer serves a critical role to separate the surface charge at the outer surface of the SiNW from the mobile charge carriers at the inner surface of the SiNW during the formation of a field effect between two surfaces. It is crucial for a passivation layer to have good properties of electrical insulation and ion-blocking to prevent electrical leakage. Also, the passivation layer should be reactive to the change of fluid pH in order to induce generation of accumulation/depletion layer of mobile charge carriers. The roles of passivation layers for electrical insulation, ion-diffusion barrier, and sensing membranes to target chemical species are significant and thus have been numerously discussed in ISFET (Ion Sensitive Field Effect Transistor)-based pH sensors [18–26]. However, previous works on SiNW pH sensors have provided only brief accounts for forming thin oxide-passivation layer by oxygen plasma [7] or short-term thermal oxidation [3–5, 9] without systematic studies of the effect of the materials and thickness on passivation layers. Either oxygen plasma or short-term thermal oxidation is not capable of accurately controlling the thickness of SiO_2 layer. Silicon dioxide (SiO_2) film has much lower dielectric constant ($\varepsilon_r = 3.9$) compared to silicon nitride (Si_3N_4) thin film ($\varepsilon_r = 7.5$) or aluminum oxide (Al_2O_3) layer ($\varepsilon_r = 9.1$). Furthermore, the diffusivity of proton ions (H^+) in SiO_2 (SiO_2

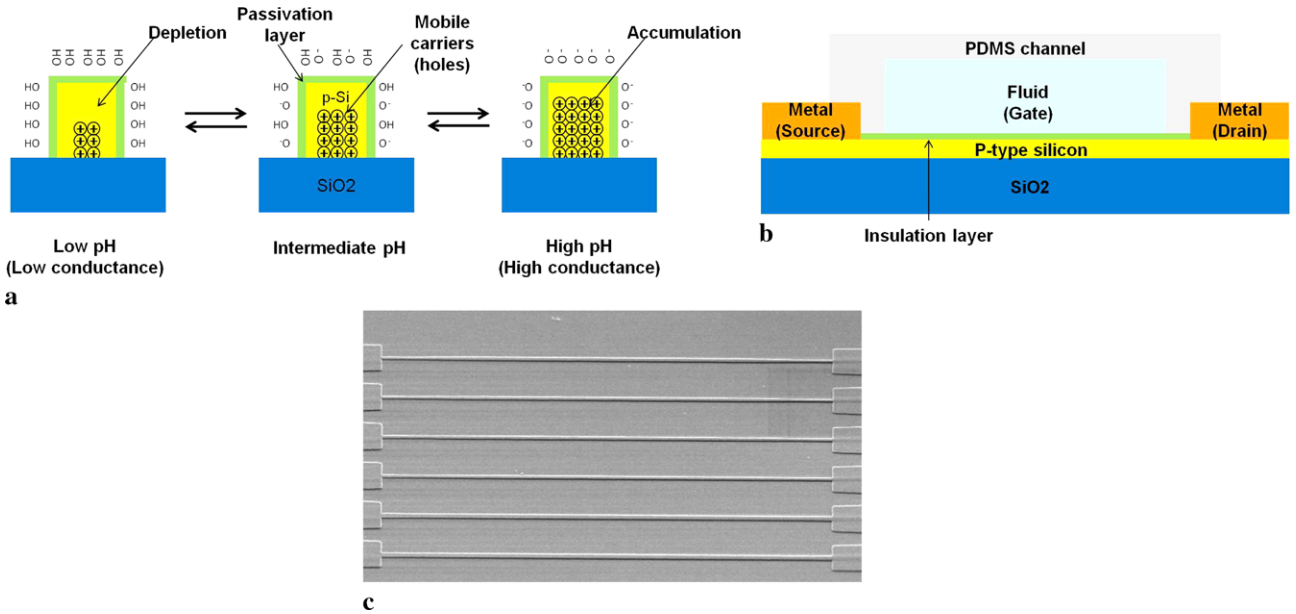

Fig. 1 Schematics of principle of pH detection/measurement. (**a**) Principle of pH detection. (**b**) Conceptual schematic of fabricated devices. (**c**) Fabricated SiNW sensor device arrays

by CVD : D = 3.3×10^{-16} cm^2/s) [19] is much higher than those of silicon nitride (by CVD : D = 10^{-19} cm^2/s) [27] or aluminum oxide (by ALD : D = 6.5×10^{-18} cm^2/s) [28].These facts imply that silicon nitride or aluminum oxide thin films can be chosen as proper passivation layers to improve electrical insulation as well as to decrease the diffusion of H^+ ions from fluid to device layer. It was previously reported that silicon nitride film [20, 23, 24, 26] and aluminum oxide film [20, 21, 25] were used as sensing membranes as well as insulation layers for pH level detection in ISFET-based sensor. In the present work, we have attempted to passivate SiNW with PECVD-based silicon nitride and to measure the stability of the sensors in different pH solutions. Also, we have characterized the pH sensitivity and the repeatability of the sensor response and interpreted the experimental results with previously reported device physics.

4 Stability of silicon nanowire-based pH sensors

The stability of the SiNW devices with various thicknesses (10, 20, and 40 nm) of silicon nitride was measured at low (pH = 4) and high (pH = 9) pH conditions for three hours. The transient responses are shown in Fig. 2. The response of the SiNW sensors with 20- and 40-nm thick silicon nitride layers shows enhanced stability which is well understood by theoretical model of the sensors in the previous literature [19]. In this model, the response of SiNW sensors with respect to time is numerically simulated by coupling and solving various governing equations of mass transport. The simulation shows that the sensor response evolves in three phases. Phase I is reaction-limited and occurs at very short time as the sensors begin to capture the analyte available very close to the surface and the response varies linearly with time. Once the region near the surface is depleted of analyte, diffusion-limited transport of analyte through water molecules dictates sensor response in phase II. Finally, in phase III, the response of the sensor saturates due to the balance of forward and backward reactions, therefore the response of the sensor is stabilized [18]. Three-hour time window is long enough to observe these three phases. In ISFET-based pH sensors, it is a well known fact that H^+ diffusion through the insulation layer causes the change of the surface state density at the interface between Si and insulator, and this change leads to a drift of sensor response [29]. Likewise, in SiNW sensors, constant supply of proton ions from fluid through thin insulation layer changes the surface state density at SiNW–insulator interface and affects the mobile carrier density which is influenced by the surface state density at the interface. We applied the principle reported in ISFET-based pH sensors [29] to explain the response of SiNW sensors. In Fig. 2, the resistance of the devices with 10-nm thick silicon nitride passivation layers decreases with unstable fluctuation in low pH and increases continuously in high pH as time passes. However, the response of the sensors with 20- and 40-nm thick silicon nitride layers quickly reaches the steady state with enhanced stability. It is speculated that the H^+ ions are not blocked by 10-nm thick silicon nitride layers and diffused into Si/insulator (i.e. nitride) interface. Under low pH conditions, H^+ ions diffuse into Si/insulator interface from the liquid solution instead of being immobilized at the outer surface of insulator and this decreases the electrostatic repulsion force between the positive charges (i.e. H^+ ions) in outer surface of insulator and holes in the inner surface of SiNW. As a result, the depletion of the mobile charge carrier (hole) is decreased and resistance of the nanowire is decreased as time proceeds. On the other hand, under high pH conditions, inherent H^+ ions which are originally present by Si/insulator interfacial defects are diffused out from the device to the fluid through silicon nitride layer and some H^+ ions are immobilized at the outer surface of insulator. This increases the electrostatic repulsion force and the region of mobile charge depletion in SiNW. As a result, the resistance of SiNW increases as the measurement time proceeds. The poor ion-blocking property of a 10-nm silicon nitride layer is caused by the defects of the layer. The defects such as pin holes or interstitial atoms are generated during PECVD processes of silicon nitride thin film [30]. When the thickness of nitride layer is increased to 20 nm, the blocking of H^+ ions is improved and shows more stable response. It is crucial to separate two contributions to transient response of the SiNW sensor: (a) long-term drift of sensor signal caused by ion diffusion from the outer surface of nitride film to the Si–nitride interface and (b) transient response caused by convective transport of ions from the solution to the outer surface of nitride film and reaction at its surface. In Fig. 2c it is observed that the resistance of the sensor with a 20-nm thick silicon nitride layer in low pH decreases during first one hour period of the measurement by the slow diffusion of H^+ ions from the solution to the silicon nitride film and reaction at the surface. After this period, the sensor response asymptotically reaches the steady state with a constant conductance since the 20-nm thick silicon nitride film serves as a good diffusion barrier against H^+ ions. Similar behavior can be observed for the response to high pH level in Fig. 2d. However, if the thickness of silicon nitride layer is only 10 nm, the SiNW sensor shows continuous decrease (at pH = 4) or increase (at pH = 9) of the response, which can be interpreted by the combined effects of ion diffusion in the liquid solution, reaction at the surface of silicon nitride film, and diffusion of ion through silicon nitride film. Short-term-noise and long-term-drift levels of the sensor responses in Fig. 2 are summarized in Table 1. Clearly, the SiNW sensor with a 10-nm thick silicon nitride layer shows unstable response with both high noise and drift levels (ex. 3 hour drift = 10.44 and −12.41% for pH = 4 and 9, respectively).

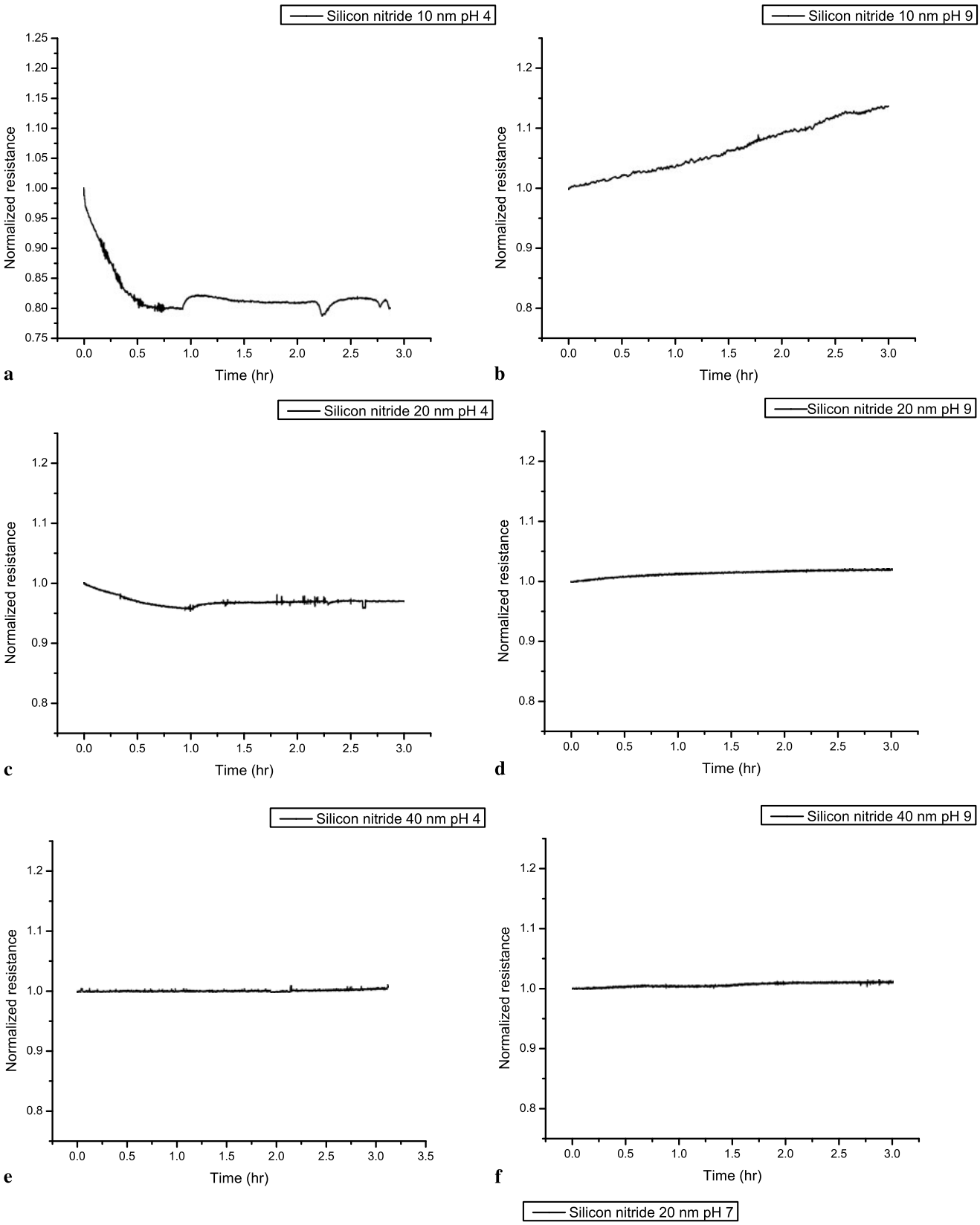

Fig. 2 Long-term (∼3 hours) electrical measurement of silicon nanowire-based pH sensor with a passivation layer of silicon nitride at low pH (pH 4) and high pH (pH 9). Normalized resistance of the device with (**a**) a 10-nm silicon nitride layer at pH 4 and (**b**) pH 9; (**c**) with a 20-nm silicon nitride at pH 4 and (**d**) pH 9; (**e**) with a 40-nm silicon nitride at pH 4 and (**f**) pH 9; and (**g**) with a 20-nm silicon nitride at pH 7

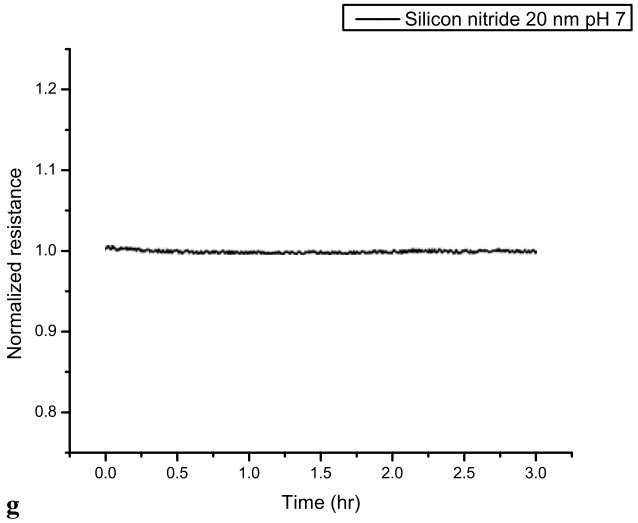

Fig. 2 (*Continued*)

However, the SiNW sensors with thicker silicon nitride layers show relatively lower noise and drift levels (ex. 3 hour drift = 0.78 and −1.68% for pH = 4 and 9, respectively). The long-term drift of these sensors was dramatically reduced as compared to previously reported data (5–6% conductance change in pH = 4 and pH = 10 for 3 hours) [9] for SiNW sensors with SiO_2 insulation layer by short thermal oxidation.

5 pH sensitivity of silicon nanowire-based pH sensors

In Fig. 3, pH response of the SiNW sensors is linear in pH 5–8. In pH 2–4, the decrease of conductance by decrease of pH level is not significant and shows nonlinear characteristics. It is speculated that the depletion of mobile carrier is saturated at strong chemical bias in very low pH. Therefore, pH 5–8 was chosen to characterize pH sensitivity of the SiNW sensor [29]. In ISFET-based pH sensors, three different mechanisms of the pH sensing are proposed: (1) Models based on the reactivity of the insulator surface. Surface sites on the insulator react with ions in the solution. This creates charge and potential in the electrical double layer in the electrolyte at the interface with the insulator. (2) Models based on the presence of mobile ions in the insulating layer. These models imply the existence of a transport mechanism, at least up to distance inside the insulator, to establish the required thermodynamic equilibrium. (3) Models based on the modification of the Si/insulator interface through a pH-controlled change in the surface state density via transport of a hydrogen-bearing species. Model (3) is an extreme form of model (2). Although the sensing output of SiNW sensors is conductance which is different from potential change in ISFET-based pH sensors, the pH sensing chemistry is still analogous with that of ISFET-based sensors. The models above are used in order to explain the measured pH response of SiNW sensors in this study. It is reported that the response time from model (1) is in the 10–100 ms range, which is much shorter than that from model (3) where a time delay in the order of several minutes to an hour is accompanied after pH change [18, 21, 23, 24, 26]. This delay effect is caused by a time lag between the depletion of analyte near the sensing surface of SiNW and the diffusion-limited transport of analyte through water molecules. Time gap between pH change and measurement timing is very critical in pH measurement in SiNW pH sensors similarly to ISFET-based pH sensors [18, 21, 23, 24, 26]. We performed the pH measurement with a short interval (5 minutes) and a long interval (3 hours) after pH step change in order to study the effect of time gap. The reproducibility of pH sensitivity of the sensor was studied as well.

Figure 3 shows that pH sensitivity of the sensor with a 20-nm silicon nitride layer is 10.85%/pH at the 1st scanning; however, this sensitivity was not reproduced in two subsequent scan cycles with 5-minute interval. After the sensor was immersed in DI water for ∼24 hours, the linear trend of pH sensitivity was reproduced at the fourth scanning, however it decreased to 5.44%/pH. This tendency was repeated in the silicon nanowire with 40-nm silicon nitride layer; the pH sensitivity of the 1st scanning was 4.51%/pH and it decreased to 2.45%/pH after DI water rinsing. The data for pH sensitivity of silicon nanowire sensors before and after DI water rinsing are summarized in Table 2. Decrease of pH sensitivity with thicker silicon nitride layer is caused by the decrease of the field effect across the insulator layer at a given chemical bias. Poor reproducibility of pH sensitivity of the sensors with short intervals is mainly attributed

Table 1 Summary of average noise level and drift level of silicon nanowire sensors at pH 4 and pH 9

Passivation layer/thickness	Average noise level (%)		Drift level (%)	
	pH 4	pH 9	pH 4	pH 9
PECVD silicon nitride/10 nm	2.49	3.44	10.44	−12.41
PECVD silicon nitride/20 nm	0.74	0.42	0.78	−1.68
PECVD silicon nitride/40 nm	0.16	0.28	−0.29	−0.90
PECVD silicon nitride/20 nm	pH 7		pH 7	
	0.36		0.24	

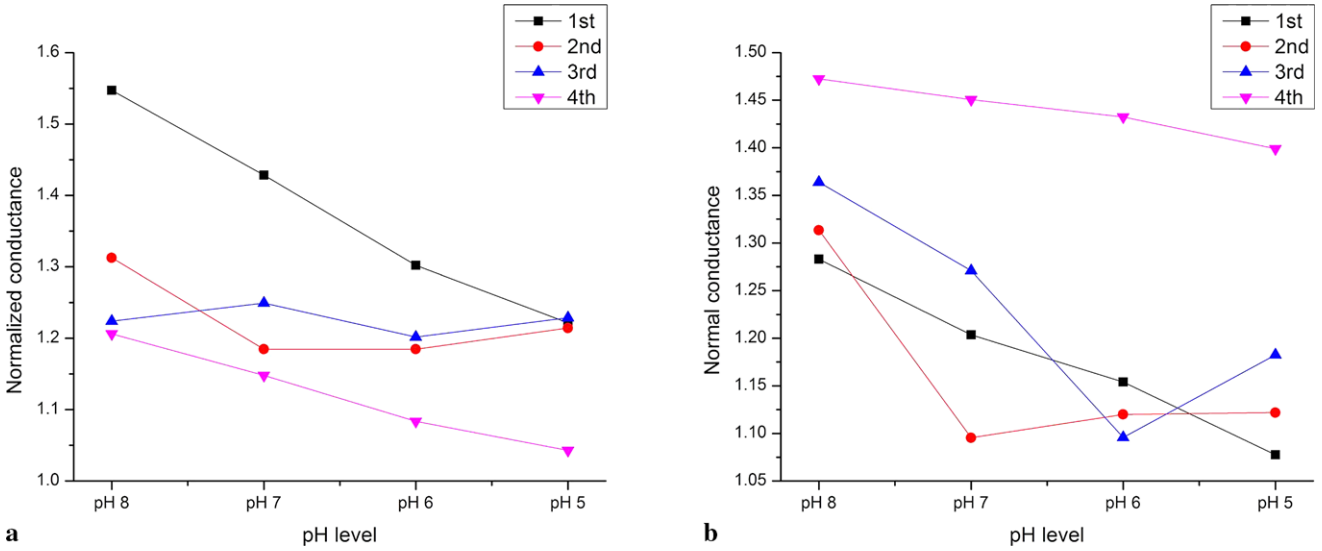

Fig. 3 pH sensitivity measurement of silicon nanowire-based pH sensor with a passivation layer of silicon nitride with a short interval (5 minutes). The 1st, 2nd, and 3rd scannings are performed in serial without water-rinsing step. The 4th scanning is performed after incubation of the sensor in water for 24 hours; (**a**) pH sensitivity measurement of the sensor with a 20-nm silicon nitride layer, and (**b**) with a 40-nm silicon nitride layer

Table 2 Summary of pH sensitivity of silicon nanowire sensors before and after DI water rinsing

Passivation layer/thickness	pH sensitivity (%/pH)	
	Before DI water rinsing	After DI water rinsing
PECVD silicon nitride/20 nm	10.85	5.44
PECVD silicon nitride/40 nm	4.51	2.45

to hysteresis (memory) effect. Even after a pH change, the effect from previous pH change still remains and interferes with the measurement of response from the current pH level. Based on the previous theoretical study [23], the width of a hysteresis loop is a function of the amplitude, time constant of the slow response, and the loop time. If the sweep time is shorter, the sensitivity decreases and a hysteresis loop increases. This theory explains the poor reproducibility shown in the 2nd and 3rd scanning. Rinsing the sensor with water for a long time period eliminates the hysteresis effect and the sensitivity is recovered at the 4th scanning. The decrease of the pH sensitivity after rinsing is caused by the surface oxidation of silicon nitride [23] and this oxidation is increased with increasing time between pH change and its measurement. The oxidation leads to the decrease of the pH sensitivity of the SiNW sensor. In this work, PECVD is used to deposit silicon nitride layer instead of Low-Pressure Chemical Vapor Deposition (LPCVD) due to the availability of equipment that is compatible to our fabrication process. In general, LPCVD-based silicon nitride layer has better ion-blocking capability than PECVD-based silicon nitride layer in ISFET devices since it generates no pin holes or interstitial atoms during the process and hydrogen is less contained than in PECVD-based silicon nitride layer. However, inherent hydrogen in silicon nitride film deposited by PECVD may have a positive effect on pH sensitivity by increasing buried OH sites on insulator layer [31]. Also, PECVD-based silicon nitride layer may have higher reactivity with proton ions and may lead to higher pH sensitivity. A study of SiNW pH sensors with LPCVD-based silicon nitride layer or Atomic Layer Deposition (ALD)-based aluminum oxide layer will be interesting subject to be explored in the future.

6 Conclusions

In this study, we developed long-term stable SiNW pH sensors by coating the SiNW with a PECVD silicon nitride-based passivation layer for effective electrical insulation and ion-blocking. The stability, pH sensitivity, and repeatability of the sensor response were systematically studied based on the physics of liquid/insulator interface and Si/insulator interface. The studies demonstrate that the sensors with a passivation layer over critical thickness ($\geq$20 nm) show long-term stability with less long-term drift response. The studies also show that there exists clear trade-off between long-term stability and pH sensitivity in silicon nanowire-based pH sensors. The sensors with thicker passivation layers over

critical thickness exhibit enhanced long-term stability but suffer from lower pH sensitivity. The detection of pH level is repeatable only after proper rinsing of sensor surfaces. It is crucial to choose a passivation layer of proper material and thickness for silicon nanowire-based pH sensors for their reliable performance in long-term pH measurement.

Acknowledgements This research is supported by the U.S. Department of Energy (DOE, Grant #: DE-AC02-05CH112), a grant (2009K000069) from the Center for Nanoscale Mechatronics & Manufacturing (CNMM), one of the 21st Century Frontier Research Programs, and Basic Science Research Program (Grant #: 2011-0004409), which are supported by Ministry of Education, Science and Technology, Korea. S. Choi thanks for his graduate fellowship from the Samsung Scholarship Foundation.

References

1. G. Zheng, W. Lu, S. Jin, C.M. Lieber, Adv. Mater. **16**, 1890–1893 (2004)
2. F. Patolsky, G. Zheng, C.M. Lieber, Anal. Chem. **78**, 4260–4269 (2006)
3. Z. Li, B. Rajendran, T.I. Kamins, X. Li, Y. Chen, R.S. Williams, Appl. Phys. A, Mater. Sci. Process. **80**, 1257–1263 (2005)
4. I. Park, Z. Li, X. Li, A.P. Pisano, R.S. Williams, Biosens. Bioelectron. **22**, 2065–2070 (2007)
5. Z. Li, Y. Chen, X. Li, T.I. Kamins, K. Nauka, R.S. Williams, Nano Lett. **4**, 245–247 (2004)
6. L.T. Canham, Nanotechnology **18**, 185704 (2007)
7. W.U. Wang, C. Chen, K.-h. Lin, Y. Fang, C.M. Lieber, Proc. Natl. Acad. Sci. USA **102**, 3208–3212 (2005)
8. Y. Cui, C.M. Lieber, Science **291**, 851–853 (2001)
9. I. Park, Z. Li, A.P. Pisano, R.S. Williams, Nanotechnology **21**, 015501 (2010)
10. Z. Fan, J.C. Ho, Z.A. Jacobson, R. Yerushalmi, R.L. Alley, H. Razavi, A. Javey, Nano Lett. **8**, 20–25 (2007)
11. D.R. Kim, C.H. Lee, X. Zheng, Nano Lett. **9**, 1984–1988 (2009)
12. D.W.-G. Alexander, Nanotechnology **17**, 4986 (2006)
13. G. Zheng, F. Patolsky, Y. Cui, W.U. Wang, C.M. Lieber, Nat. Biotechnol. **23**, 1294–1301 (2005)
14. P.J. Pauzauskie, A. Radenovic, E. Trepagnier, H. Shroff, P. Yang, J. Liphardt, Nat. Mater. **5**, 97–101 (2006)
15. D.K. Schroder, *Semiconductor Material and Device Characterization* (IEEE Press/Wiley, Hoboken, 2006)
16. J.-P. Colinge, C.-W. Lee, A. Afzalian, N.D. Akhavan, R. Yan, I. Ferain, P. Razavi, B. O'Neill, A. Blake, M. White, A.-M. Kelleher, B. McCarthy, R. Murphy, Nat. Nanotechnol. **5**, 225–229 (2010)
17. B.G. Streetman, S. Banerjee, *Solid State Electronic Devices* (Pearson/Prentice Hall, Upper Saddle River, 2006)
18. P.R. Nair, M.A. Alam, *Performance Limits of Nanobiosensors*, vol. 88 (AIP, New York, 2006)
19. D. Fink, J. Krauser, D. Nagengast, T.A. Murphy, J. Erxmeier, L. Palmetshofer, D. Bräunig, A. Weidinger, Appl. Phys. A, Mater. Sci. Process. **61**, 381–388 (1995)
20. M. Yuqing, G. Jianguo, C. Jianrong, Biotechnol. Adv. **21**, 527–534 (2003)
21. L. Bousse, D. Hafeman, N. Tran, Sens. Actuators B, Chem. **1**, 361–367 (1990)
22. L. Bousse, S. Mostarshed, B. van der Schoot, N.F. de Rooij, Sens. Actuators B, Chem. **17**, 157–164 (1994)
23. L. Bousse, H.H. van den Vlekkert, N.F. de Rooij, Sens. Actuators B, Chem. **2**, 103–110 (1990)
24. R. Kenhold, H. Ryssel, Sens. Actuators B, Chem. **68**, 307–312 (2000)
25. M.J. Schoning, D. Tsarouchas, L. Beckers, J. Schubert, W. Zander, P. Kordos, H. Ltith, Sens. Actuators B, Chem. **35**, 228–233 (1996)
26. J. Chou, Y. Tseng, Proc. SPIE **4078**, 793 (2000)
27. G.T. Yu, S.K. Yen, Surf. Coat. Technol. **166**, 195–200 (2003)
28. G.C. Yu, S.K. Yen, Appl. Surf. Sci. **201**, 204–207 (2002)
29. N.F. de Rooij, P. Bergveld, Thin Solid Films **71**, 327–331 (1980)
30. J.C. Knights, R.A. Lujan, M.P. Rosenblum, R.A. Street, D.K. Bieglesen, J.A. Reimer, Appl. Phys. Lett. **38**, 331–333 (1981)
31. L. Bousse, P. Bergveld, Sens. Actuators **6**, 65–78 (1984)